LWT - Food Science and Technology 216 (2025) 117302

Contents lists available at ScienceDirect

LWT

journal homepage: www.elsevier.com/locate/lwt

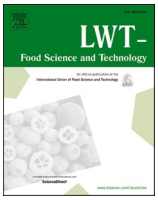

Evaluation of biomarkers that influence the freshness of beef during storage using VIS/NIR hyperspectral imaging

Azfar Ismail [a,b,1], Seongmin Park [c,d,1], Hye-Jin Kim [a], Minwoo Choi [a], Hyun-Jun Kim [a], Heesang Hong [a], Ghiseok Kim [c,d,**], Cheorun Jo [a,d,e,*]

[a] Department of Agricultural Biotechnology and Center for Food and Bioconvergence, Seoul National University, Seoul, 08826, Republic of Korea
[b] Microalgae-Biota Technology and Innovation Group (ALBIC), Department of Aquaculture, Faculty of Agriculture, Universiti Putra Malaysia, 43400, Serdang, Selangor, Malaysia
[c] Department of Biosystems Engineering, Seoul National University, Seoul, 08826, Republic of Korea
[d] Research Institute of Agriculture and Life Sciences, Seoul National University, Seoul, 08826, Republic of Korea
[e] Institute of Green Bio Science and Technology, Seoul National University, Pyeongchang, 25354, Republic of Korea

ARTICLE INFO

Keywords:
Beef aging
Metabolite profiling
Hyperspectral imaging
Partial least squares regression
Biomarkers correlation

ABSTRACT

Biomarkers influencing the freshness of beef during storage were detected using VIS/NIR hyperspectral imaging (HSI). A total of 18 cuts of eye round from three cattle were vacuum-packaged and wet-aged at 4 ± 2 °C for 27 days. Throughout this period, freshness was maintained as evidenced by a significant decrease in pH, stable color, and total bacterial count (TBC) and volatile basic nitrogen (VBN) remaining below spoilage thresholds at 5.78 Log CFU/g and 14.47 mg/100 g, respectively. Metabolite profiling revealed correlations between freshness indicators-ethanol, 5′-inosine monophosphate, acetate, histamine-and TBC and VBN values, highlighting their importance in freshness. Integrating HSI with partial least squares regression (PLSR) proved more reliable than artificial neural networks for predicting metabolite profiles and correlating them with quality traits, confirming its effectiveness in meat quality monitoring. With PLSR, the model performance for TBC was similar ($R^2 = 0.77$ from HSI and 0.74 from metabolite predictions), while VBN performance improved significantly from $R^2 = 0.63$ to 0.81 with predicted metabolite data. This integration was essential for monitoring beef quality during wet aging and for developing effective assessment strategies.

1. Introduction

Beef, renowned for its rich content of high-quality proteins, essential amino acids, and abundant vitamins, is highly susceptible to enzymatic and microbial decomposition throughout its production and distribution stages (Bergen, 2021). This susceptibility leads to a decline in freshness, marked by significant deteriorating changes resulting from both internal reactions within the beef and interactions with external organisms (Liu et al., 2019). Beyond diminishing its quality and nutritional value, this degradation raises concerns about safety and erodes consumer confidence. Consequently, monitoring beef freshness becomes paramount to safeguarding consumers and ensuring food security (Liu et al., 2022a; Hu, et al., 2022).

The freshness of beef is vulnerable to biochemical, physicochemical, and microbiological changes, marking the initiation of deterioration. Microorganisms play a pivotal role by breaking down proteins through proteolytic activity, resulting in the formation of free amino acids (Xu et al., 2023). There is potential for meat spoilage through the metabolic activities of various proliferating microorganisms. This metabolic process involves oxidative deamination, decarboxylation, and desulfurization, producing metabolites such as NH_3, CO_2, and H_2S, which contribute to off-odors and spoilage. For instance, lactic acid bacteria generate lactic acid when they interact with the carbon source in meat (Costa et al., 2019). This interaction induces protein precipitation, microbial protection, and a pH decrease, imparting an acidic taste (Antonelo et al., 2020). Therefore, identifying specific metabolites and bacterial spoilage is critical for assessing meat freshness, as both are highly correlated.

* Corresponding author. Research Institute of Agriculture and Life Sciences, Seoul National University, Seoul, 08826, Republic of Korea.
** Corresponding author. Research Institute of Agriculture and Life Sciences, Seoul National University, Seoul, 08826, Republic of Korea.
E-mail addresses: ghiseok@snu.ac.kr (G. Kim), cheorun@snu.ac.kr (C. Jo).
[1] These authors contributed equally.

https://doi.org/10.1016/j.lwt.2024.117302
Received 29 July 2024; Received in revised form 23 December 2024; Accepted 27 December 2024
Available online 4 January 2025

One specific indicator of microbial degradation in food proteins is volatile basic nitrogen (VBN) as stated by Biji et al. (2015). The increase of VBN during meat storage is attributed to the breakdown of muscle proteins into amino acids by enzymes secreted by microorganisms. The elevated VBN and other freshness indicators in meat are closely linked to glucose depletion (Uwimbabazi et al., 2017). This phenomenon underscores a microbial shift toward protein breakdown for energy, resulting in VBN production and microbial effects (Xu et al., 2023). Despite extensive research on this mechanism, the interpretation of VBN and total bacteria count (TBC) in beef studies remains limited, particularly in connecting their content with metabolite biomarkers (Bekhit et al., 2021; Xu et al., 2023).

Traditional methods for evaluating beef freshness are often time-consuming, expensive, require specialized personnel, and are destructive (Eom et al., 2014; Ma et al., 2019). The complex metabolites and chemical composition of meat further complicate assessment, necessitating advanced techniques (Hassoun et al., 2020). Hyperspectral imaging (HSI) is an emerging tool that captures spectral information across the entire sample, providing a three-dimensional data cube of two-dimensional spatial images and one-dimensional spectra. HSI allows for the analysis of physical properties like shape, color, and size, and the prediction of chemical composition using mechanical models (Cheng et al., 2018). Embracing accurate, non-destructive, and rapid identification methods is crucial for maintaining supply chain integrity (Jia et al., 2022).

In recent years, the HSI techniques have garnered attention for their capabilities in beef freshness evaluation, providing high analytical efficiency and simultaneous analysis of multiple indicators (Jia et al., 2022). Although extensively studied in meat products, its application for beef metabolites correlated to the chemical and biological mechanisms is yet to be explored. This introduction highlights the challenges in beef production, the complexities of assessing freshness, and the potential of advanced technologies like HSI for real-time monitoring. The hypothesis is that HSI can serve as a reliable, non-destructive, and efficient tool for monitoring beef freshness by accurately detecting and analyzing metabolite compounds associated with freshness indicators. Therefore, this study aimed to combine HSI with traditional methods to investigate metabolite compounds associated with the freshness of refrigerated beef, correlating the results with VBN and TBC.

2. Materials and methods

2.1. Sample preparation

A total of 18 cuts of eye round from three cattle were purchased from three different butcher shops, with each animal originating from a different farm in South Korea. The cuts, each measuring 7 cm × 7 cm × 4 cm, were vacuum-packaged using a polyethylene/nylon bag (with an oxygen permeability of 22.5 mL/m^2/24 h atm at 60% relative humidity (RH)/25 °C and a water vapor permeability of 4.7 g/m^2/24 h at 100% RH/25 °C) using an HFV-600L machine (Hankook Fujee Machinery Co., Ltd., Hwaseong, Korea). The packaged cuts were then stored at 4 ± 2 °C for 1, 7, 14, 16, 20, and 27 days prior to analysis.

2.2. Microbiological and physicochemical traits

2.2.1. Microbiological analysis

Total bacterial count (TBC) was conducted according to Ismail et al. (2023) and International Commission on Microbiological Specifications for Foods guidelines. Ten grams of sample were aseptically sliced from the surface and promptly transferred to a sterile bag containing 90 mL of 0.85% NaCl solution. The sample was mixing using a BagMixer 400P (Interscience Ind., St. Nom, France), serial dilutions were performed to obtain countable concentrations. Subsequently, 1 mL aliquots of appropriate dilution were inoculated on plate count agar (Difco Laboratories, Detroit, MI, USA). The agar plate was incubated at 37 °C for 48 h, and then colonies were counted as Log CFU/g.

2.2.2. Volatile basic nitrogen (VBN)

The VBN content was determined following the methods by Ismail et al. (2023). Three grams of sample were homogenized with 27 mL of distilled water using an Ultra-118 Turrax T25 homogenizer (Ika-Werke, Staufen, Germany) at 9500 rpm for 30 s. The homogenates were then centrifuged at 2265×*g* for 10 m using a Union 32R centrifuge (Hanil) and filtered through Whatman No. 1 filter paper (Whatman plc, Maidstone, UK). Subsequently, 1 mL of each sample, 50% K_2CO_3, and 0.01N H_3BO_3, along with 100 μL of the indicator (0.066% methyl red in ethanol: 0.066% bromocresol green in ethanol, 1:1, w/v), were added to a Conway unit (Sibata Ltd., Sitama, Japan). The Conway unit was then sealed and incubated at 37 °C for 1 h using a DS-130L incubator (Daewon Sci. Co., Bucheon, Korea). After incubation, color changes were observed and recorded by adding 0.01 N HCl to the center of the Conway, and VBN was calculated using the provided formula.

$$\text{VBN (mg/100 g of sample)} = 0.14 \times (V1 - V0) \times 10 \times 100 \div S$$

Where, V1 denotes the volume of 0.01 N HCl added in the treatment group, while V0 represents the volume added in the control group. S represents the weight of the sample, and 0.14 signifies the amount of volatile basic nitrogen per milliliter of 0.01N HCl solution.

2.2.3. pH value

Three grams of each sample were homogenized with 27 mL of distilled water using a homogenizer (Ultra-Turrax T25, Ika-Werke, Staufen, Germany) at 1720×*g* for 30 s. The homogenates were then centrifuged (Union 32R, Hanil, Seoul, Korea) at 2265×*g* for 10 min and filtered (Whatman No. 4, Whatman plc, Maidstone, UK). The pH of each filtrate was measured using a pH meter (SevenGo, Mettler-Toledo, Schwerzenbach, Switzerland).

2.2.4. Meat color

Meat color assessment was performed using a colorimeter (CM-5, Konica Minolta Sensing Inc., Osaka, Japan). The observer angle was set at 10°, with illuminant D_{65} and standard illuminant C. The blooming process of meat was exposed to outside for 30 min prior to measurement. Meanwhile the colorimeter was calibrated using a standard white plate. A white standard plate was referred to the International Commission of Illumination (CIE); CIE $L^* = 96.79$, CIE $a^* = 0.30$, and CIE $b^* = 1.67$. L^*, a^*, b^*, C^* and h, representing lightness, redness, yellowness, chroma and hue angle, respectively. Each sample was analyzed five times, and the mean value was considered a single replicate.

2.3. Metabolite profiles

Metabolite extraction was conducted with five replicates per treatment and sampling day, following the method explained by Ismail et al. (2024) with minor modifications. Five grams of the sample underwent extraction using 20 mL of 0.6 M perchloric acid with a homogenizer (Ultra-Turrax T25, Ika-Werke) at 1720×*g* for 1 min. The resulting homogenates were then centrifuged (Union 32R, Hanil) at 2265×*g* for 20 min and subsequently filtered. The pH of the homogenate sample was tuned to 7 ± 0.01 using 0.6 M perchloric acid and 10 mM phosphate buffer before centrifugation under the previous conditions. Each resulting supernatant was filtered (Whatman No. 1, Whatman plc) and then subjected to lyophilization (Freezer dryer 18, Labconco, Kansas City, MO, USA). The lyophilized sample was reconstituted with deuterium oxide (D_2O) containing 1 mM 3-(trimethylsilyl) propionic-2,2,3,3-d4 acid (TSP) to quantify metabolites. The reconstituted sample was incubated in a water bath at 35 °C for 10 min, followed by cooling for another 10 min. After centrifugation, 1 mL of the supernatant was transferred to a 2 mL Eppendorf tube and centrifuged again at 17,000×*g* for 10 min. Subsequently, 600 μL supernatant was transferred into an

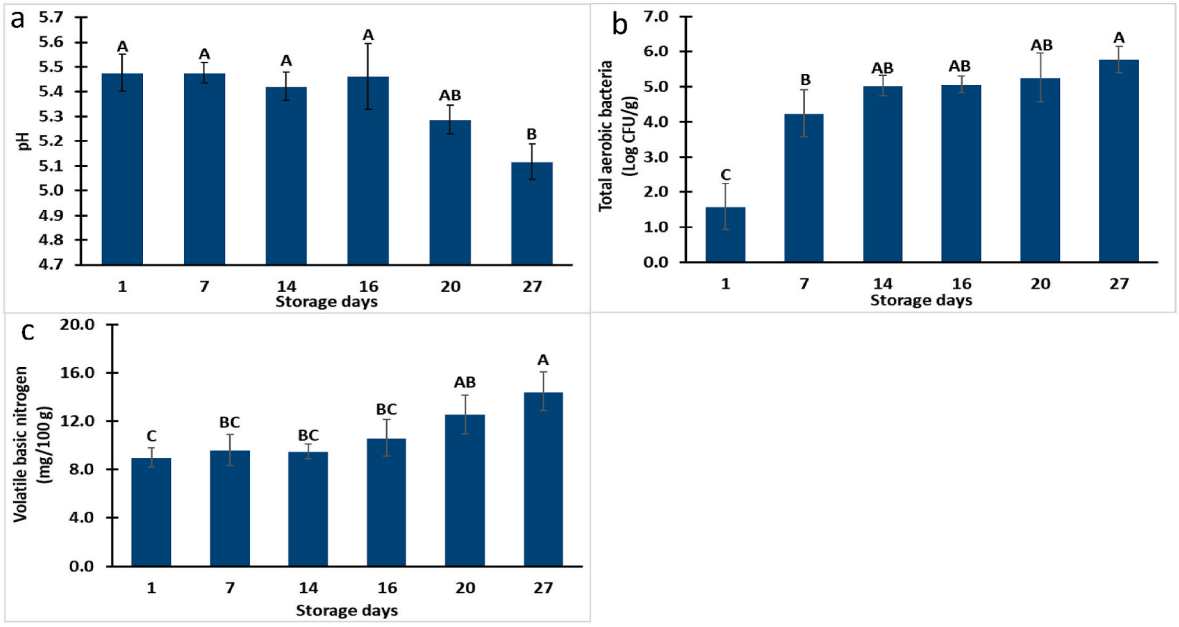

Fig. 1. Quality traits of (a) pH value, (b) total bacterial count in Log CFU/g, and (c) volatile basic nitrogen (mg/100 g) in refrigerated beef during storage. Differences in superscripts A-C indicate statistically significant differences between storage days ($p < 0.05$).

NMR tube.

One-dimensional ^{1}H nuclear magnetic resonance (NMR) and ^{1}H–^{13}C heteronuclear single quantum coherence (HSQC) spectra were recorded at 298 K on a Bruker 850 MHz cryo-NMR spectrometer by AVANCE III HD (Bruker Biospin GmbH, Rheinstetten, Germany). Lock, tune, and shimming procedures were performed automatically. Following acquisition, spectra underwent processing using a modified standard zg30 pulse sequence (recycle delay of 1 s) provided by the default program in Topspin 3.6.2 (Bruker Biospin GmbH), with lock on the D_2O deuterium resonance. The 1D ^{1}H NMR experiment utilized 64 k data points and a sweep width of 17,006.803 Hz with 128 scans, while the ^{1}H–^{13}C HSQC was analyzed using 512 increments in T1 with 8 scans and 2 k data points in the T2 domain. Manual phase correction and peak integration were performed. Metabolite identification relied on chemical shift comparison with the Human Metabolome Database (HMDB) (www.hmdb.ca) using Chenomx NMR Suite 7.1 software (Chenomx, Edmonton, Canada). Metabolites in each sample were identified by comparing their peak assignments with those in the HMDB library. The resonance of TSP served as the internal standard for calibration and comparison of chemical shifts (δ) in the sample. The concentration of metabolites was quantified using the following equation below:

$$Concentration\ (mg/kg) = \left[Numbers\ of\ proton\ (internal\ standard) Numbers\ of\ proton\ (metabolite) \times Intensity\ of\ peak\ (metabolite) \times Intensity\ of\ peak\ (internal\ standard) \times Internal\ standard\ concentration\ (1\ mM/mL) \times Molar\ mass\ \left(\frac{mol}{kg}\right) \right] \div sample\ volume$$

2.4. HSI system and data acquisition

HSI analysis was conducted utilizing a push-broom scanner equipped with an HSI-200 sensor (Korea Spectral Products, Seoul, Korea). To ensure complete elimination of external light, an image acquisition system was set up in a dark environment. The HSI system included an imaging spectrometer with a resolution of 640 spectral × 512 spatial, utilizing an InGaAs imaging sensor covering the spectrum from visible to short-wave near-infrared regions. Tungsten halogen lamps provided sample illumination to ensure uniform lighting during imaging. Each image pixel contained 640 wavelengths, spanning from 278 to 1724 nm.

The beef samples were cut into replicates measuring 3 × 3 × 1 cm (width × length × height), with a total of 144 samples (6 storage days × 3 animals × 8 observations) analyzed. The samples were allocated into a training dataset for validation approach due to the limited number of samples collected. A Teflon whiteboard with 99.99% reflectivity was utilized to obtain the white reference, while the dark reference was acquired by covering the camera to achieve 0% reflectance. This procedure aimed to eliminate the dark current effect and minimize the impact of uneven illumination, resulting in normalized reflectance data within the range of 0–1. The normalized reflectance data were calculated using the following equation (Ismail et al., 2024).

$$Reflectance\ (\%) = (Intensity\ of\ sample - Signal\ intensity\ of\ dark\ reference) \div (Signal\ intensity\ of\ white\ reference - Signal\ intensity\ of\ dark\ reference)$$

After constructing the reflectance data, each spectrum included in the region of interest of the same sample was processed. After the preprocessing method was applied, the final spectral data for each image were averaged and compared with the reference data. From the reflectance data, wavelengths identified as outliers were considered noise and subsequently removed. Therefore, the final spectral range was from 400 to 1600 nm.

The obtained metabolite profiles and spectral data were compared by PLSR based on multivariate analysis and artificial neural network (ANN) based on machine learning. PLSR compresses the data into a few latent variables that contain the most information from both input and output

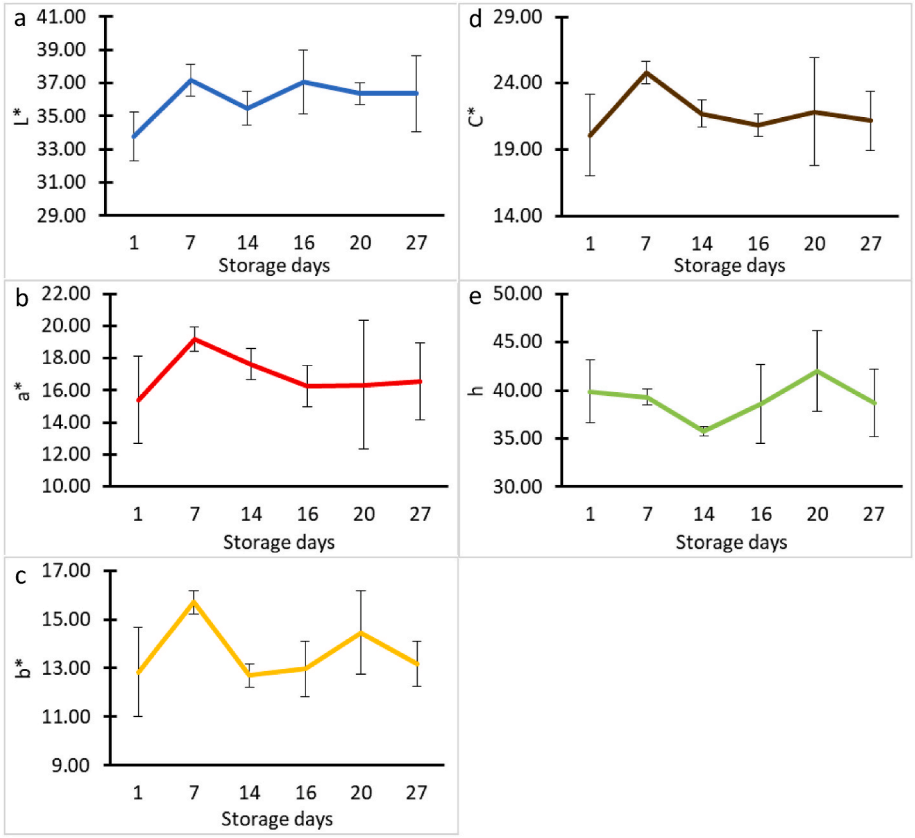

Fig. 2. CIE color measurements of (a) Lightness, *L**, (b) Redness, *a**, (c) Yellowness, *b**, (d) Chroma, *C**, and (e) Hue angle, h of refrigerated beef during storage. *Storage: 1, 7, 14, 16, 20 and 27 days.

variables in the data set and performs least squares regression. The optimal number of components for the model must be determined on the spot. For each metabolite profile, the model was developed by varying the number of components from 1 to 40, selecting the number of components that yielded the lowest RMSE value, using both the X-matrix generated from the spectral data and the Y-vector generated from the measured metabolite profiles.

As a machine learning technique, ANN learns the optimal neuron structure to produce the given results without explicitly programming general classification rules. Typically, a considerable amount of trial and error is required to determine the optimal ANN topology (Curteanu & Cartwright, 2011). In this research, for each metabolite profile, six models with one or two hidden layers and node numbers of 25, 30, and 35 in each layer were tested to determine the best performing model. The activation function used for the hidden layers was ReLU (rectified linear unit), and the optimizer used during the compilation process was Adam (adaptive momentum estimation).

2.5. Statistical analysis

The data underwent analysis using a one-way ANOVA and Tukey's test with a significance level of 95%, conducted through the SAS 9.4 program (SAS Institute Inc., Cary, NC, USA). The data is presented as the mean (n = 3 animals) along with the standard error of the mean. Multivariate and correlation analyses were carried out using MetaboAnalyst 5.0 (www.metaboanalyst.ca) following the methodology outlined by Kim et al. (2023). Additionally, principal component analysis (PCA) and partial least squares-discriminant analysis (PLS-DA) were employed to identify the metabolites contributing to the separation of samples based on storage duration. VIP scores were derived from the PLS-DA results, serving as indicators of the metabolites significantly influencing sample separation. Prior to analysis, samples underwent log transformation and auto-scaling. The HSI dataset was utilized to construct PLS models using Python version 3.8.5 (Python Software Foundation, Wilmington, USA).

3. Results and discussion

3.1. Microbiological and physicochemical traits

Fig. 1 illustrates the observed trends in refrigerated beef, highlighting significant changes in pH, TBC and VBN. Specifically, the pH levels exhibited a decreasing trend over time, reaching the lowest point of 5.12 on day 27 compared to the initial value of 5.48 (Fig. 1a). The pH value nearing the isoelectric point of structural proteins, influenced by calpain activity, led to denaturation or degradation of the proteins during beef aging. Consequently, the capillaries between actin and myosin filaments lost their capacity to retain water (Liu et al., 2022b). Meanwhile the TBC and VBN showed an increasing trend throughout the storage period (Fig. 1b and c).

On day 27, a significant decrease was observed in pH (5.12), and a significant increase was found in both TBC (5.78 Log CFU/g) and VBN (14.47 mg/100 g) compared to other storage days of beef. Low pH on day 27 had increased lactic acid bacteria, which helps inhibit spoilage and maintain beef quality (Hui et al., 2023). Despite these fluctuations, it is notable that both TBC and VBN remained below the threshold limit for spoilage, suggesting that, overall, the beef quality was within acceptable limits. Even though there were substantial changes in the quality indicators on day 27, the beef managed to maintain its overall quality without exceeding spoilage limits. The TBC data from the current study was lower than that from the previous studies. For instance, in a study by Kukhtyn et al. (2020), 16-day beef stored at 0 ± 0.5 °C had a TBC of 8.5 Log CFU/cm^2. Meanwhile, the VBN value in beef during 21-day storage was lower than the spoilage threshold value for meat in

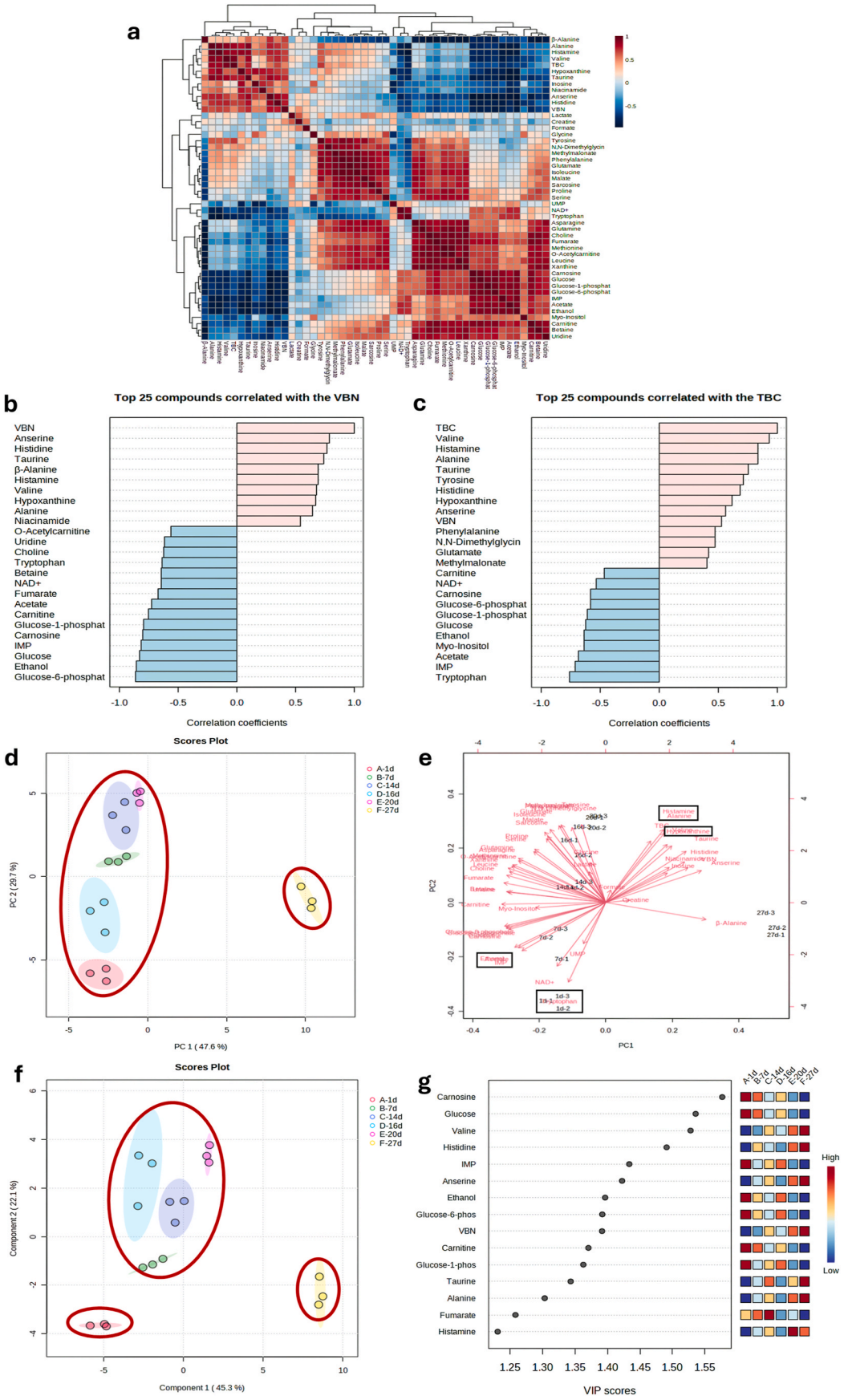

Fig. 3. Change of metabolites of refrigerated beef during storage of (a) Correlation heatmap of metabolites, total bacterial count (TBC), and volatile basic nitrogen (VBN) (b) Correlation coefficients of metabolites with VBN, (c) Correlation coefficients of metabolites with TBC, (d) Score plot by PCA, (e) Biplot by PCA, (f) Score plot by PLS-DA, and (g) VIP scores by PLS-DA.

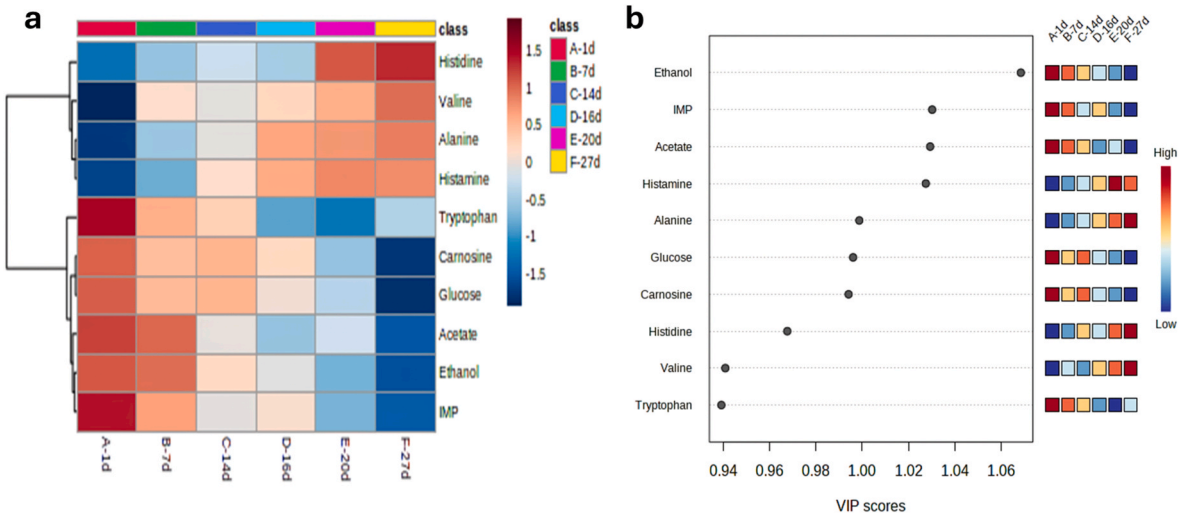

Fig. 4. Selected 10 metabolites based on the correlation coefficient ($r > 0.6$ and $r < -0.6$) in both total bacterial count and volatile basic nitrogen of (a) Heatmap and (b) VIP scores, obtained from the refrigerated beef during storage.

Korea, which is 20 mg/100 g, with values exceeding this considered as spoilage (Yu et al., 2020).

The color attributes, encompassing *L**, *a**, *b**, *C** and h, revealed intriguing patterns as shown in Fig. 2. On day 7, these color parameters reached their peak, signifying an increase in all color space representation during the storage. However, as the beef aging period in the refrigerator progressed beyond day 7, there was a subsequent decline and fluctuation in these color attributes. This change could be attributed to various factors such as microbial activity, oxidation processes, and enzymatic reactions affecting the meat quality over time (Domínguez et al., 2019; Katiyo et al., 2020). This suggests that the meat experienced a subsequent reduction in CIE colors over time (Hui et al., 2023).

As shown Fig. 2, the color instability increased from day 2 precisely *L**, *a**, and *b** values had decreased with muscle color changing from bright red to dark red. This may be due to the loss of pigment resulting from the oxidation of myoglobin and oxymyoglobin to methemoglobin (Sen et al., 2014). Despite this deterioration, it was observed that these changes were not statistically significant across the entire storage period. As a result, the meat's color stability was preserved, with only minor fluctuations in CIE color values throughout the aging period. The insignificant differences in CIE colors imply that the overall color quality of the beef remained relatively consistent, supporting the chemical and biological properties indicative of acceptable quality throughout the storage days (Hui et al., 2023).

3.2. Correlation of metabolites with quality findings

Fig. 3a illustrates the correlation heatmap of various metabolites, TBC, and VBN. An increase in TBC and VBN showed a decrease in amino acids. Elevated levels of VBN, encompassing ammonia, dimethylamine (DMA), and trimethylamine (TMA), alongside microorganisms, act as indicators of microbial protein decay in meat products (Bekhit et al., 2021). Numerous bacteria consumed high energy for metabolism and amino acid catabolism in meat (Kwon et al., 2022). In addition, biosynthesis of non-essential amino acids like alanine, valine, and tyrosine was produced from the synthesis process of living organisms. Meanwhile, VBN is associated with the protein degradation of meat (Domínguez et al., 2022). In this finding, flavor from nucleotides were notably correlated with VBN, such as histamine, hypoxanthine, and inosine. Nucleotides, serving as carriers of energy in the form of triphosphates, play crucial roles in various cellular processes and provide the energy required for protein synthesis and other cellular activities (Dong et al., 2020).

The bar graph further validated the association of metabolites with freshness by correlating them with VBN and TBC among the top 23 metabolites found in refrigerated beef. The highest correlation with VBN was observed for anserine (positive correlation) and glucose-6-phosphate (negative correlation), as shown in Fig. 3b. The results in agreement with previous findings by Kwon et al. (2022), showing a correlation between VBN and the levels of anserine and glucose. This consistency supports the hypothesis that these compounds are crucial in the metabolic processes involving VBN. Meanwhile, TBC exhibited the highest correlation with valine (positive correlation) and tryptophan (negative correlation), as shown in Fig. 3c. Among the compounds correlated with VBN and TBC, ten were specifically chosen based on their excellent correlation coefficients ($r > 0.6$ and $r < -0.6$). These crucial compounds included histidine, valine, alanine, histamine, tryptophan, carnosine, glucose, acetate, ethanol, and IMP. All these compounds were correlated with the meat freshness precursors during storage (Ismail et al., 2024).

All ten selected compounds were further analyzed in this study (Fig. 4). Upon heatmap analysis, it became evident that day 27 exhibited higher levels of end-products of metabolism associated with decreased freshness compared to other storage days (Fig. 4a). The levels of histidine, valine, alanine, and histamine increased, while the remaining selected compounds contradicted on day 27 of beef aging (Mohammed et al., 2020). Notably, among the selected metabolites, ethanol, IMP, acetate, and histamine stood out with the highest VIP scores (>1.02), signifying their important roles in distinguishing the deteriorated condition observed on day 27 (Fig. 4b). In addition, the levels of histamine, which was among the selected metabolites, peaked on day 20 and showed a subsequent decrease on day 27. This pattern might be attributed to potential competition among histamine-producing bacteria with other dominant microorganisms or increased metabolism facilitated by endogenous enzymes capable of metabolizing histamine in the meat (Hua et al., 2018).

The decrease in ethanol, acetate and IMP during storage is due to microbial fermentation, indicating microbial activity from spoilage microorganisms (Hwang et al., 2022). These microorganisms metabolize carbohydrates, producing ethanol as a byproduct, eventually decreasing over time (Hwang et al., 2022). Similarly, acetate, a metabolic byproduct, accumulates during meat storage and is produced by microorganisms such as lactic acid and acetic acid bacteria (Shewail et al., 2018). The presence of ethanol and acetate can affect meat flavor and aroma, sometimes imparting a sour taste linked to spoilage. The decrease in ethanol and acetate levels indicates slower microbial activity

Table 1
A total of 49 metabolites values predicted using partial least squares regression and artificial neural networks obtained from hyperspectral imaging.

Metabolites	PLSR		ANN	
	R-Square	RMSE	R-Square	RMSE
Acetate	0.73	2.10	0.63	2.62
Alanine	0.64	9.89	0.51	12.10
Anserine	0.69	3.76	0.34	5.59
Asparagine	0.46	0.32	0.46	0.33
Betaine	0.53	4.07	0.37	4.67
Carnitine	0.51	40.47	0.34	46.56
Carnosine	0.63	6.59	0.39	8.54
Choline	0.62	10.00	0.28	13.62
Creatine	0.21	57.68	0.21	57.89
Ethanol	0.73	1.98	0.54	2.54
Formate	0.25	0.37	0.05	0.44
Fumarate	0.58	1.80	0.24	2.43
Glucose-1-phosphate	0.46	1.22	0.49	1.27
Glucose-6-phosphate	0.55	11.26	0.45	12.77
Glucose	0.59	15.46	0.44	18.56
Glutamate	0.69	5.41	0.33	7.98
Glutamine	0.54	8.59	0.28	10.71
Glycine	0.52	3.85	0.19	5.49
Histamine	0.75	0.47	0.58	0.61
Histidine	0.58	0.78	0.31	1.00
Hypoxanthine	0.70	7.19	0.54	9.34
IMP	0.66	11.05	0.55	12.64
Inosine	0.69	2.71	0.34	4.01
Isoleucine	0.74	6.08	0.38	9.60
Lactate	0.27	104.25	0.09	117.29
Leucine	0.63	10.67	0.21	15.59
Malate	0.58	3.03	0.48	3.51
Methionine	0.57	2.96	0.22	4.06
Methylmalonate	0.63	0.88	0.22	1.31
Myo-Inositol	0.55	6.11	0.37	7.05
N,N-Dimethylglycine	0.61	0.48	0.23	0.69
NAD+	0.75	0.36	0.35	0.59
Niacinamide	0.43	0.54	0.46	0.50
O-Acetylcarnitine	0.53	5.32	0.41	5.99
Phenylalanine	0.70	5.01	0.37	7.60
Proline	0.42	0.94	0.26	1.09
Sarcosine	0.74	1.09	0.54	1.52
Serine	0.57	3.09	0.15	4.71
Taurine	0.68	5.47	0.43	7.20
Tryptophan	0.85	0.12	0.63	0.20
Tyrosine	0.72	3.46	0.43	5.15
UMP	0.64	1.58	0.37	1.99
Uridine	0.53	0.24	0.31	0.30
Valine	0.68	4.97	0.48	6.29
Xanthine	0.64	1.84	0.31	2.60
β-Alanine	0.53	0.56	0.33	0.66
TBC	0.77	0.66	0.63	0.81
VBN	0.45	1.63	0.42	1.67

and spoilage over time, making them valuable markers for monitoring meat quality (Lee et al., 2023). IMP levels fluctuate during storage due to enzymatic and microbial activities, with further degradation leading to the formation of inosine and hypoxanthine, which are associated with reduced taste and quality (Dong et al., 2020).

Fig. 3d shows the score plot by principal component analysis (PCA), revealing two distinct groups, categorizing the samples into fresh (1, 7, 14, 16, and 20 days) and less fresh (27 days). Meanwhile, the biplot illustrates specific compounds influencing beef freshness, with a strong positive correlation observed for histamine, hypoxanthine, alanine, and histidine, and a strong negative correlation noted for IMP, tryptophan, ethanol, and acetate (Fig. 3e). This trend aligns with the theory of metabolites deterioration in meat during storage (Lee et al., 2023). However, when compared with partial least square-discriminant analysis (PLS-DA) in Fig. 3f, the score plot improved, demonstrating three precise groups: very fresh (1 day), fresh (7, 14, 16, and 20 days), and less fresh (27 days). The differentiation of the 1-day storage of meat was particularly notable.

No spoilage was found, which can be attributed to the TBC and VBN of the meat remaining below the threshold limits during the 27 days of refrigerator storage. The standard values should be below 7 Log CFU/g and 20 mg/100g, respectively, as stated by the International Commission on Microbiological Specifications for Foods and the Korean Ministry of Agriculture and Forestry for standardization of quality control. The PLS-DA illustrates the VIP scores of beef metabolites during storage (Fig. 3g). Carnosine had the highest VIP scores, exceeding 1.55, followed by glucose, valine, histidine, IMP, and anserine with scores surpassing 1.40. The values for carnosine, glucose, and IMP were lowest on day 27 of meat storage, while valine, histidine, and anserine exhibited their highest values. The findings were linked to the increase in VBN values observed on the same day. These results are also consistent with the heatmap correlations and the biplot analysis, as discussed earlier. Additionally, histamine, alanine, and ethanol also showed high VIP scores, each exceeding 1.0.

Overall, the correlation between metabolite findings with TBC and VBN values highlights their significance in distinguishing beef freshness. Specific metabolites such as ethanol, IMP, acetate, and histamine are crucial indicators of beef freshness during storage. The fluctuations of these metabolites during storage reflect microbial activity and enzymatic processes affecting meat quality. PCA and PLS-DA analyses effectively differentiated beef samples over 27 days by identifying two to three groups of freshness (very fresh, fresh, and less fresh). Interestingly, no spoilage was detected in beef stored over 27 days, as TBC and VBN remained below threshold limits. Key metabolites, including carnosine, glucose, valine, histidine, IMP, and anserine, emerged as highly significant indicators of beef freshness, as demonstrated through detailed metabolomic analysis. These metabolites play crucial roles in the biochemical processes that change as freshness declines, with their levels providing clear and measurable signals of quality. The study's insights into these mechanisms underscore how shifts in these metabolite concentrations can reliably indicate the freshness status, making them valuable markers for assessing beef quality. Key metabolites, including carnosine, glucose, valine, histidine, IMP, and anserine, emerged as highly significant indicators of beef freshness. The values of these metabolites play crucial roles in the biochemical processes that change as freshness fluctuates found in VBN and TBC from this study, providing clear and measurable signals of quality. The mechanisms underscore how shifts in these metabolite values can reliably indicate the freshness status, making them valuable markers for assessing beef quality. From this investigation, it is recommended to store vacuum-packaged beef in the refrigerator for up to 20 days without additional preservation methods to maintain optimal freshness and quality.

3.3. Integration of spectral modeling with metabolite findings

The spectral modeling in predicting metabolite profiles reinforces earlier findings on key metabolites such as ethanol, IMP, acetate, and histamine, which are crucial indicators of beef freshness. The correlation of TBC and VBN with spectral data highlights the significance of microbial activity and metabolite fluctuations in assessing meat quality (Byun et al., 2003). This approach enhances metabolomic studies by integrating metabolite findings with spectral data analysis for effective freshness monitoring (Ismail et al., 2023). The HSI model, employed with multivariate analysis, demonstrated a strong correlation with quality and metabolite findings, validating its use in freshness assessment.

Metabolite correlation analysis is commonly utilized to identify components present in each spectrum, employing various techniques including traditional principal component analysis (PCA), PLSR, multiple linear regression (MLR), and deep learning (Ismail et al., 2024). Table 1 shows the performance of prediction models using Partial Least Squares Regression (PLSR) and Artificial Neural Network (ANN) techniques to match spectral modelling from hyperspectral imaging (HSI) data with corresponding metabolite profiles, providing prediction performance for each of the 49 metabolites for comparison. Notably, TBC

Table 2
Average metabolite models using total bacterial count (TBC) and volatile basic nitrogen (VBN) values as feature parameters without spectral data.

PLSR				ANN			
TBC		VBN		TBC		VBN	
R-Square	RMSE	R-Square	RMSE	R-Square	RMSE	R-Square	RMSE
0.68	0.63	0.62	1.25	0.16	2.23	0.21	2.30

Table 3
Performance of models using hyperspectral imaging data to predict average metabolites with total bacterial count (TBC) and volatile basic nitrogen (VBN).

PLSR						ANN					
TBC			VBN			TBC			VBN		
N	R-Square	RMSE	N	R-Square	RMSE	N	R-Square	RMSE	N	R-Square	RMSE
30	0.74	0.63	25	0.81	0.93	25	0.28	1.67	40	0.17	2.70

N, the number of selected metabolites.

exhibited higher correlations in both PLSR and ANN ($R^2 = 0.63–0.77$) compared to other metabolite values. This is attributed to the unique optical properties of bacteria, which are more readily detected using spectroscopy (Byun et al., 2003).

The PLSR model showed better prediction performance than ANN model for almost all metabolites. Specifically, acetate, ethanol, histamine, isoleucine, NAD+, phenylalanine, sarcosine, tyrosine, and TBC showed higher correlations in PLSR, exceeding 0.7, with tryptophan achieving the highest value at 0.8471. In contrast, acetate exhibited the highest correlation in spectral data using ANN ($R^2 = 0.63$; RMSE = 2.62) compared to other beef metabolites. This variability may be attributed to factors such as limited sample size, inherent data complexity, and differences in reference data values (Ismail et al., 2023; Wang et al., 2023).

The better performance of the PLSR model over the ANN model can be attributed to factors such as multicollinearity and the amount of training data (Garg & Tai, 2013). This superior performance of PLSR also highlights the robustness of PLSR in handling linear relationships within the spectral data. PLSR is particularly adept at handling data with linear relationships, while ANN thrives on capturing complex patterns in nonlinear data. From this viewpoint, it can be assumed that the PLSR analysis performed well because the data analyzed in this study had hidden linearity. Also, the feature that PLSR can derive effective models from comparatively small data sets, while ANN generally requires extensive training data, may have influenced the results.

Table 2 illustrates the performance of average metabolites matching models with TBC and VBN values treated as feature parameters without using spectral data. Notably, PLSR for TBC demonstrated a significantly higher correlation coefficient ($R^2 = 0.68$) compared to ANN ($R^2 = 0.16$). Similar findings were found for VBN whereby significantly higher correlation coefficient using PLSR ($R^2 = 0.62$) compared to ANN ($R^2 = 0.21$). These results underscore the utility of PLSR in capturing variations associated with TBC and VBN. Therefore, showing the robustness of PLSR findings aligns with previous research utilizing this model with HSI in the context of metabolites matching models. PLSR is considered to have high performance because it effectively exploits the high correlations between features present in meat spectral data (Aït-Kaddour et al., 2020). In contrast, ANN may experience performance degradation on such data because it does not explicitly consider the correlations between features.

Table 3 presents the performance of models using spectral data to predict the average metabolites and then utilizing these feature parameters to predict TBC and VBN values. The number of predicted metabolites was selected based on the results in Table 1, and the models with the highest R-squared value were chosen. Such predictions can be beneficial when experimental data for metabolite profiles are unavailable. It is common for this dual-prediction structure to perform worse due to the iterative nature of the predictions, and this research is consistent with that. Even with this method, PLSR had more reliable results in the correlation of total data with TBC and VBN. While ANN provided unreliable data, combining other machine learning methods such as support vector machine and random forest, or using ensemble models through bagging and boosting techniques could lead to better results. Therefore, model performance of TBC was similar between 0.77 (from HSI data, Table 1) and 0.74 (from predicted metabolites data by HSI data, Table 3). However, model performance of VBN was strongly improved from 0.63 (from HSI data, Table 1) to 0.81 (from predicted metabolites data by HSI data, Table 3).

4. Conclusion

The comprehensive analysis of refrigerated beef encompassing microbiological, physicochemical traits, and metabolite profiles yielded valuable insights into its quality preservation during storage. Despite observing variations in pH, TBC and VBN values over time, the beef has consistently maintained its quality within acceptable standards, highlighting the efficacy of the storage conditions employed. The investigation into freshness revealed a correlation between TBC, VBN, and various metabolites based on fundamental biochemical processes in beef, particularly on day 27 of storage. Analysis of color attributes revealed stable color quality throughout the storage duration, with no significant deviations noted across different days. Furthermore, the investigation into metabolite profiles revealed strong and significant links between TBC, VBN, and a range of key metabolites, offering valuable understanding into the complex biochemical processes that govern beef freshness. These findings were especially striking on day 27 of storage, highlighting critical shifts in metabolite concentrations that directly influence beef quality, underscoring the depth and importance of these biochemical interactions. Moreover, the integration of HSI with PLSR demonstrated high reliability in linking metabolite data with TBC and VBN, thereby reinforcing its utility in quality assessment. The integration of HSI with traditional methods was found to be crucial for comprehending beef quality changes during refrigerated storage, thus guiding the development of optimal storage to maintain freshness and quality.

CRediT authorship contribution statement

Azfar Ismail: Writing – original draft, Investigation, Formal analysis, Conceptualization. **Seongmin Park:** Writing – original draft, Investigation, Formal analysis, Conceptualization. **Hye-Jin Kim:** Writing – review & editing, Methodology, Data curation. **Minwoo Choi:** Writing – review & editing, Formal analysis. **Hyun-Jun Kim:** Writing – review & editing, Formal analysis. **Heesang Hong:** Writing – review & editing, Formal analysis. **Ghiseok Kim:** Writing – review & editing, Validation, Supervision, Project administration. **Cheorun Jo:** Writing –

review & editing, Validation, Supervision, Project administration, Funding acquisition.

Declaration of competing interest

The authors declare that they have no known competing financial interests or personal relationships that could have appeared to influence the work reported in this paper.

Acknowledgments

This work was supported by the Korea Evaluation Institute of Industrial Technology (KEIT, 20012411).

Data availability

Data will be made available on request.

References

Aït-Kaddour, A., Andueza, D., Dubost, A., Roger, J. M., Hocquette, J. F., & Listrat, A. (2020). Visible and near-infrared multispectral features in conjunction with artificial neural network and partial least squares for predicting biochemical and microstructural features of beef muscles. *Foods, 9*(9), 1254. https://doi.org/10.3390/foods9091254

Antonelo, D., Gómez, J. F., Cônsolo, N. R., Beline, M., Colnago, L. A., Schilling, W., Zhang, X., Suman, S. P., Gerrard, D. E., Balieiro, J. C., & Silva, S. L. (2020). Metabolites and metabolic pathways correlated with beef tenderness. *Meat and Muscle Biol, 4*(1), 1–9. https://doi.org/10.22175/mmb.10854

Bekhit, A. E.-D. A., Giteru, S. G., Holman, B. W. B., & Hopkins, D. L. (2021). Total volatile basic nitrogen and trimethylamine in muscle foods: Potential formation pathways and effects on human health. *Comprehensive Reviews in Food Science and Food Safety, 20*(4), 3620–3666. https://doi.org/10.1111/1541-4337.12764

Bergen, W. G. (2021). Amino acids in beef cattle nutrition and production. In G. Wu (Ed.), *Amino acids in nutrition and health. Adv. Exp. Med. Biol.* (Vol. 1285). Cham: Springer. https://doi.org/10.1007/978-3-030-54462-1_3.

Biji, K. B., Ravishankar, C. N., Mohan, C. O., & Srinivasa Gopal, T. K. (2015). Smart packaging systems for food applications: A review. *J. Food Sci. Technol, 52*, 6125–6135. https://doi.org/10.1007/s13197-015-1766-7

Byun, J.-S., Min, J. S., Kim, I. S., Kim, J.-W., Chung, M.-S., & Lee, M. (2003). Comparison of indicators of microbial quality of meat during aerobic cold storage. *J. Food Protect., 66*(9), 1733–1737. https://doi.org/10.4315/0362-028x-66.9.1733.

Cheng, G., Li, Z., Han, J., Yao, X., & Guo, L. (2018). Exploring hierarchical convolutional features for hyperspectral image classification. *IEEE Trans. Geosci. Remote Sens., 56*(11), 6712–6722. https://doi.org/10.1109/TGRS.2018.2841823

Curteanu, S., & Cartwright, H. (2011). Neural networks applied in chemistry. I. Determination of the optimal topology of multilayer perceptron neural networks. *Journal of Chemometrics, 25*(10), 527–549. https://doi.org/10.1002/cem.1401

Domínguez, R., Pateiro, M., Gagaoua, M., Barba, F. J., Zhang, W., & Lorenzo, J. M. (2019). A comprehensive review on lipid oxidation in meat and meat products. *Antioxidants, 8*(10), 429. https://doi.org/10.3390/antiox8100429

Domínguez, R., Pateiro, M., Munekata, P. E. S., Zhang, W., Garcia-Oliveira, P., Carpena, M., Prieto, M. A., Bohrer, B., & Lorenzo, J. M. (2022). Protein oxidation in muscle foods: A comprehensive review. *Antioxidants, 11*(1), 1–24. https://doi.org/10.3390/antiox11010060

Dong, M., Qin, L., Ma, L.-X., Zhao, Z.-Y., Du, M., Kunihiko, K., & Zhu, B.-W. (2020). Postmortem nucleotide degradation in turbot mince during chill and partial freezing storage. *Food Chemistry, 311*, Article 125900. https://doi.org/10.1016/j.foodchem.2019.125900

Eom, K.-H., Hyun, K.-H., Lin, S., & Kim, J.-W. (2014). The meat freshness monitoring system using the smart RFID tag. *Int. J. Distrib. Sens. Netw., 10*(7). https://doi.org/10.1155/2014/591812

Garg, A., & Tai, K. (2013). Comparison of statistical and machine learning methods in modelling of data with multicollinearity. *Int. J. Model. Identif., 18*(4), 295–312. https://doi.org/10.1504/IJMIC.2013.053535

Hassoun, A., Måge, I., Schmidt, W. F., Temiz, H. T., Li, L., Kim, H.-Y., Nilsen, H., Biancolillo, A., Aït-Kaddour, A., Sikorski, M., et al. (2020). Fraud in animal origin food products: Advances in emerging spectroscopic detection methods over the past five years. *Foods, 9*, 1069. https://doi.org/10.3390/foods9081069

Hua, H., Li, Y., Liang, J., & Fred, D. F. (2018). Molecular regulation of histamine synthesis. *Frontiers in Immunology, 9*, 1392. https://doi.org/10.3389/fimmu.2018.01392

Hui, T., Fang, Z., Ma, Q., Hamid, N., & Li, Y. (2023). Effect of cold atmospheric plasma-assisted curing process on the color, odor, volatile composition, and heterocyclic amines in beef meat roasted by charcoal and superheated steam. *Meat Science, 196*, Article 109046. https://doi.org/10.1016/j.meatsci.2022.109046

Hwang, S. H., Lee, J., Nam, T. G., Koo, M., & Cho, Y. S. (2022). Changes in physicochemical properties and bacterial communities in aged Korean native cattle beef during cold storage. *Food Sci. Nutr., 10*, 2590–2600. https://doi.org/10.1002/fsn3.2864

Ismail, A., Lee, H. J., Hong, S.-J., Kim, G., Choi, M., & Jo, C. (2024). Evaluation of plasma-activated lactic-gallic acid treated chicken meats on the freshness, volatile changes, and metabolites through multi-analytical techniques. *Innov. Food Sci. Emerg. Technol., 91*, Article 103544. https://doi.org/10.1016/j.ifset.2023.103544

Ismail, A., Ryu, J., Yim, D. G., Kim, G., Kim, S. S., Lee, H. J., & Jo, C. (2023). Quality evaluation of mackerel fillets stored under different conditions by hyperspectral imaging analysis. *Food Sci. Anim. Resour., 43*(5), 840–858. https://doi.org/10.5851/kosfa.2023.e39

Jia, W., van Ruth, S. M., Scollan, N. D., & Koidis, A. (2022). Hyperspectral Imaging (HSI) for meat quality evaluation across the supply chain: Current and future trends. *Current Research in Food Science, 5*, 1017–1027. https://doi.org/10.1016/j.crfs.2022.05.016

Katiyo, W., de Kock, H. L., Coorey, R., & Buys, E. M. (2020). Sensory implications of chicken meat spoilage in relation to microbial and physicochemical characteristics during refrigerated storage. *LWT, 128*, Article 109468. https://doi.org/10.1016/j.lwt.2020.109468

Kukhtyn, M., Salata, V., Berhilevych, O., Malimon, Z., Tsvihun, A., Gutyj, B., & Horiuk, Y. (2020). Evaluation of storage methods of beef by microbiological and chemical indicators. *Potr. S.J.F. Sci., 14*, 602–611. https://doi.org/10.5219/1381

Kwon, J. A., Yim, D.-G., Kim, H.-J., Ismail, A., Kim, S.-S., Lee, H. J., & Jo, C. (2022). Effect of temperature abuse on quality and metabolites of frozen/thawed beef loins. *Food Sci. Anim. Resour., 42*(2), 341–349. https://doi.org/10.5851/kosfa.2022.e9

Lee, D., Kim, H.-J., Ismail, A., Kim, S.-S., Yim, D.-G., & Jo, C. (2023). Evaluation of the physicochemical, metabolomic, and sensory characteristics of Chikso and Hanwoo beef during wet aging. *Anim. Biosci., 36*(7), 1101–1119. https://doi.org/10.5713/ab.23.0001

Liu, J., Ellies-Oury, M. P., Stoyanchev, T., & Hocquette, J. F. (2022a). Consumer perception of beef quality and how to control, improve and predict it? Focus on eating quality. *Foods, 11*(12), 1732. https://doi.org/10.3390/foods11121732

Liu, J., Hu, Z., Zheng, A., Ma, Q., & Liu, D. (2022b). Identification of exudate metabolites associated with quality in beef during refrigeration. *LWT, 172*, Article 114241. https://doi.org/10.1016/j.lwt.2022.114241

Liu, H., Saito, Y., Riza, D. F., Kondo, N., Yang, X., & Han, D. (2019). Rapid evaluation of quality deterioration and freshness of beef during low temperature storage using three-dimensional fluorescence spectroscopy. *Food Chemistry, 287*, 369–374. https://doi.org/10.1016/j.foodchem.2019.02.119

Ma, J., Sun, D. W., Pu, H., Cheng, J. H., & Wei, Q. (2019). Advanced techniques for hyperspectral imaging in the food industry: Principles and recent applications. *Annual Review of Food Science and Technology, 10*, 197–220. https://doi.org/10.1146/annurev-food-032818-121155

Mohammed, H. H., Jin, G., Ma, M., Khalifa, I., Shukat, R., Elkhedir, A. E., Zeng, Q., & Noman, A. E. (2020). Comparative characterization of proximate nutritional compositions, microbial quality and safety of camel meat in relation to mutton, beef, and chicken. *LWT, 118*, Article 108714. https://doi.org/10.1016/j.lwt.2019.108714

Sen, A. R., Naveena, B. M., Muthukumar, M., & Vaithiyanathan, S. (2014). Colour, myoglobin denaturation and storage stability of raw and cooked mutton chops at different end point cooking temperature. *J. Food Sci. Technol., 51*(5), 970–975. https://doi.org/10.1007/s13197-011-0557-z

Shewail, A., Shaltout, F., & Gerges, T. (2018). Impact of some organic acids and their salts on microbial quality and shelf life of beef. *Assiut Veterinary Medical Journal, 64*(159), 164–177. https://doi.org/10.21608/avmj.2018.169040

Uwimbabazi, E., Mukasekuru, M. R., & Sun, X. (2017). Glucose biosensor based on a glassy carbon electrode modified with multi-walled carbon nanotubes-chitosan for the determination of beef freshness. *Food Analytical Methods, 10*(8), 2667–2676. https://doi.org/10.1007/s12161-017-0793-6

Xu, L., Liu, S., Cheng, Y., & Qian, H. (2023). The effect of aging on beef taste, aroma and texture, and the role of microorganisms: A review. *Crit. Rev. Food Sci., 63*(14), 2129–2140. https://doi.org/10.1080/10408398.2021.1971156

Yu, H. H., Kim, Y. J., Park, Y. J., Shin, D.-M., Choi, Y.-S., Lee, N.-K., & Paik, H.-D. (2020). Application of mixed natural preservatives to improve the quality of vacuum skin packaged beef during refrigerated storage. *Meat Science, 169*, Article 108219. https://doi.org/10.1016/j.meatsci.2020.108219